J Sol-Gel Sci Technol (2013) 68:19–30
DOI 10.1007/s10971-013-3129-z

ORIGINAL PAPER

Preparation of three-component TEOS-based composites for stone conservation by sol–gel process

Rong Liu · Xiangna Han · Xiao Huang · Weidong Li · Hongjie Luo

Received: 21 February 2013 / Accepted: 28 July 2013 / Published online: 7 August 2013

Abstract Tetraethoxysilane (TEOS) is the most commonly used silicon-based stone consolidant in art conservation. However, it is known that the resulting silica gel phase tends to develop cracks inside the stone as the gel shrinks during aging and drying. Such phenomenon may lead to severe damage to the protected objects. By introducing silica nanoparticles into TEOS, a so-called particle modified consolidant (PMC), may minimize such shrinkage by reducing the volume loss and forming mesoporous structure to weaken the capillary forces. But many previous results show significant color changes on the surface of PMC-treated stones which can not be tolerated in the conservation treatments of cultural heritage. In this work, we designed a three-component composite consolidant which consists of 15 nm silica particles, α,ω-hydroxyl-terminated polydimethylsilane (PDMS-OH) and TEOS. Among the three components, TEOS provides the consolidation function, silica nanoparticles prevent the cracking and increase the salt resistance and PDMS-OH further reduces cracking, decreases the color alteration and increases the resistance to wetting of the stone. Experimental results show that the three components have significant synergistic effect, which makes the material exhibiting best overall performance in terms of cultural heritage protection.

Keywords Sol–gel · Silica nanoparticles · TEOS · Polydimethylsilane · Stone consolidation

R. Liu · X. Han · X. Huang (✉)
State Key Laboratory of High Performance Ceramics and Superfine Microstructures, Shanghai Institute of Ceramics, Chinese Academy of Sciences, Shanghai 200050, China
e-mail: xiaohuang@mail.sic.ac.cn

R. Liu · X. Han · W. Li · H. Luo (✉)
Key Scientific Research Base of Ancient Ceramic, Shanghai Institute of Ceramics, Chinese Academy of Sciences, Shanghai 200050, China
e-mail: hongjieluo@mail.sic.ac.cn

H. Luo
Shanghai University, Shanghai 200436, China

1 Introduction

Stone relics such as historical buildings and grottoes located outdoors are exposed to the risk of being damaged by severe degradation, due to weathering and human activities over the years [1]. The stone will lose its strength with time, and if no external actions are taken, the precious relics will disappear forever. Conservation of stone objects is a delicate and complex problem [2]. Actually, the consolidation treatment is fairly risky in restoration, because the action itself is irreversible, regardless of the products used. But consolidation is still widely applied because of its practical feasibility. Among numerous materials applied in art conservation, the organosilanes such as alkoxy- or alkyl-alkoxysilane-based consolidants, due to their unique molecular structures, have shown promising results and attracted a lot of attention [3].

Most commercial consolidants applied to restore the strength of the weathered stone are in the forms of sols or solutions. The liquids can be drawn into the pores of the stone by capillary forces easily, where they solidify via gelation and/or drying processes [4]. The earliest organosilane consolidants applied are tetraethoxysilane (TEOS) and its oligomers [5]. Even nowadays, TEOS and its oligomers are still the main components among the complex formulations of a series of commercial products for restoration. Their advantages are well known: the low

viscosity, the ability to form silicon–oxygen (Si–O–Si) bonds [6]. The silicon–oxygen bond is the major chemical bonding form in many of the minerals, which contributes to the compatibility between organosilane and the stone. Low viscosity and high affinity to the minerals allow the liquid to transport easily inside the stone, wet the stone surface well and penetrate into a certain depth [7].

Tetraethoxysilane and its oligomers can react with the moisture in the air to form stable gels with a silicon–oxygen backbone within the stone's inter-granular network [8]. The silicon oxide gel network can function as a binder as the original binder in the stone has been lost during weathering, leading to significant enhancement of the cohesion and adhesion among the stone grains [9]. Thus the stone's mechanical strength can be improved effectively after consolidation treatment. Unlike organic polymers, silicon–oxygen bonds in silica are quite stable and have excellent resistance to aging, which makes TEOS and its oligomers very attractive for outdoor use [5].

However, there is a serious drawback of simple alkoxysilanes like TEOS as consolidant, which has been recognized and carefully studied—the resulting silica gel phase, as the gel shrinks, tends to develop cracks inside the stone due to the stress generated from significant mass and volume losses and increasing capillary force during aging and drying [10–12]. Such problem has been a great challenge and a major research focus in stone consolidation applications. Conservare OH®, a commercial stone consolidant which is developed to reduce crack formation in stone consolidation, has shown significant improvement in many practical applications. But due to the complexity of the stone objects and applying conditions and protocols, there are still many reported unsatisfied results using Conservare OH® as consolidant [13]. Thus, continuing research to solve the cracking issue is still of great importance and in urgent demand.

Several approaches have been adopted to suppress cracking during drying [14–18]. One promising way is to prepare the so-called particle-modified consolidants (PMC) by introducing colloidal oxides such as silica into the alkoxysilane consolidants [19]. The addition of nanoparticles will reduce the overall mass loss and volume shrinkage to restrain the cracking since there is no volatiles coming from nanoparticles [20]. Meanwhile, the addition of nanoparticles can significantly change the gel's pore structure, i.e., enlarge the pore sizes leading to smaller capillary stress since the capillary forces are inversely proportional to the pore radius [7]. Besides diminishing crack formation, PMC can also improve stone resistance to wetting [21] and salt damage [22].

But with all the benefits PMC can provide, in many cases, it has been observed that PMC can notably change the appearance of the stone due to the high refraction index of the solid particles [20]. Previous reports show that the total color difference ΔE (CIE L*a*b* color space) of TiO_2-PMC can be as high as 29, while ΔE of Al_2O_3-PMC and SiO_2-PMC are 8.0 and 7.4 respectively [21], which is totally unacceptable. The total color difference ΔE before and after consolidation treatment for conservation of cultural heritage should be <5 [23]. Overall, such severe appearance changes must be corrected before wide application of PMC in stone consolidation.

Polydimethylsiloxane (PDMS) is a very common silicon-based polymer. Unlike the silica network formed from TEOS which is very brittle, the two methyl groups and elastic chains in PDMS can provide extra flexibility to the network [24]. The incorporation of PDMS into the TEOS-based stone consolidant network can also minimize the cracking without obvious color alteration [25]. The hydrophobic nature of PDMS will improve the water resistance of the stone objects as well. But the aging of PDMS may be a concern [26], and to the best of our knowledge, such an issue has not been carefully examined in stone consolidation applications.

This paper reports the preparation and evaluation of a three-component silicon-based stone consolidant, which consists of α,ω-hydroxyl-terminated PDMS (PDMS-OH), silica nanoparticles and TEOS. In the initial designation, among the three components, TEOS will provide the consolidation function and act as a base material. Silica nanoparticles will restrain the crack formation and improve the resistance to aging and salt. Meanwhile PDMS-OH will further suppress cracking formation while reducing the color alteration caused by silica nanoparticles. Based on the laboratory evaluation, through the synergistic effect of the three components, our silicon-based consolidants show overall best performance on stone conservation.

2 Experimental section

2.1 Materials

Tetraethoxysilane (AP, Shanghai Lingfeng Co.), isopropanol (≥99.7 %, Shanghai Lingfeng Co.), PDMS-OH (MW 400–700, 4–6 % terminal OH, Meryer), SiO_2 nanoparticles (99.5 %, 15 ± 5 nm, Aladdin), and di-*n*-butyltindilaurate (DBTL, 95 %, Aladdin) were used as received. The DBTL is used as a neutral catalyst.

Sandstone samples were from the quarry near the Big Buddhist Temple in Shaanxi province, China, whose major component is quartz (61.01 wt% SiO_2 and 10.91 wt% Al_2O_3). It also contains up to 2.59 wt% Fe_2O_3, which gives it the well-known dark red appearance. Before usage, the sandstones were cut into 20 × 20 × 20 mm^3 cubic blocks, 40 × 40 × 10 mm^3 slabs and 20 × 20 × 200 mm^3

columns respectively. And then all samples were cleaned by sonication in deionized water for an hour before being dried in an oven at 110 °C for 4 h.

2.2 Instrumentation

Viscosities were measured by a Brookfield viscometer (model DV-II with UL/Y adapter, rotor S18, 150RPM) at 20 °C controlled by a circulating water bath (CH2015, Shanghai Fangrui). Photos were taken by a Canon G12 digital camera. Scanning electron micrographs (SEM) were recorded on a HITACHI S-4800 scanning electron microscope. Chromium alloy was vacuum evaporated onto the samples. Nitrogen adsorption isotherms and pore size distribution of xerogels were measured by Micromeritics ASAP3020. The overall porosity and pore size distribution were also characterized by mercury intrusion porosimetry (MIP, AutoPore 9500). Compressive strength was measured by an Instron 5592 universal testing machine. Dynamic elastic modulus (E) was measured using a commercial instrument (Xiangke Co., China). The water absorption experiment was carried out by a ceramic absorb water ratio determining tester (Xiangyi, China). The static contact angle θ of the surfaces of the untreated and treated samples were measured by contact angle meter (JC2000C, Powereach, equipped with a video camera). Color alteration was monitored by a Konica Minolta CM 2600d spectrophotometer. A hydrostatic balance (Mokeli Co., China) was used to weight the sample in water.

2.3 Consolidant sol preparation and sol–gel process

Five samples named S, SP1, SP2, SP3, and P as well as a control sample are listed in Table 1. The overall chemical content in all samples is controlled to be as close as possible. TEOS without addition of silica nanoparticles or PDMS is used as control.

Certain amounts of silica nanoparticles and/or PDMS were first dispersed/dissolved in isopropanol for 120 min sonication (KH5200DE ultrasonic cleaner, Kunshan Hechuang Co.). Then, weighed amount of TEOS was added into the isopropanol dispersions under magnetic agitation. Each mixture was homogenized by sonication for 10 min before deionized water (molar ratio of TEOS/H_2O = 1/4) was added dropwisely. After completion of water addition, the reactants were stirred for another hour, and then 1 wt% of DBTL was added. Finally, all samples were kept at 40 °C for 4 h under magnetic stirring for the sol–gel process to proceed. The viscosity of each sol was immediately measured after preparation. For comparison, the viscosity of pure TEOS was also measured.

Table 1 Composition of the composite consolidant sols

SOLS	Nano silica (wt%)	PDMS (wt%)	TEOS (wt%)	Total percentage of all chemicals (wt%)
Control	0	0	22	22
S	4	0	18	22
SP1	4	1	18	23
SP2	2	1	20	23
SP3	1	1	20	22
P	0	1	22	23

The gelation and following drying process of the sols were examined in bulk and films separately. 2 mL of each consolidant sol was poured into a plastic dish with a diameter of 4 cm, and then covered by parafilm with pinholes. 4 mL of consolidant sol was sealed in a plastic test tube with pinholes on the cap for solvent evaporation [27]. All samples were kept in a temperature humidity chamber to gel (T = 25 °C, RH = 50 %, SETH-Z-022R, ESPEC).

2.4 Consolidation evaluation

Direct capillary absorption is a more reliable procedure for stone protection, but full immersion method is more convenient and practical in laboratories [28]. Full immersion method is applied in the present work. Sandstone samples were soaked in consolidant sols (Control, S, SP1, SP2, SP3 and P) for 24 h. Then all samples were placed in the temperature humidity chamber (T = 25 °C, RH = 50 %) for at least 4 weeks until sol–gel process finished. The sol–gel process was considered to be complete when the sample's weight difference of two consecutive measurements, which were taken every 24 h, was <0.001 g.

The effect of consolidation is demonstrated by compressive strength, measured according to ASTM C170/C170M-09 [29].

The water absorption experiment was carried out using the gravimetric method [30]. First, the sample was completely immersed in deionized water at room temperature in a cylindrical chamber, and then the chamber was sealed and vacuumed for 15 min to de-gas the sample completely. The chamber remained closed for at least 30 min for water to saturate the stone samples before them being taken out. The samples were wiped with tissue paper carefully to remove any surface water and weighted immediately. Afterwards, all the water saturated specimens were weighted again in water by using a hydrostatic balance in order to calculate the open porosity. The water uptake and open porosity were calculated based on the following equations: [30]

$$\text{Water uptake}(\%) = \frac{W_1 - W_0}{W_0} \times 100 \quad (1)$$

$$\text{Open porosity}(\%) = \frac{W_1 - W_0}{W_1 - W_2} \times 100 \quad (2)$$

In both equations, W_0 is the original mass of the stone sample while W_1 and W_2 are the mass of the stone after water saturation measured in air and water respectively. Three treated stone samples ($20 \times 20 \times 20$ mm^3) were used for each consolidant. Data reported were average of three individual samples.

Vapor permeability was evaluated following the Deutsche Industrie Normen 52615 procedure [31]. Treated and untreated samples were cut into $40 \times 40 \times 10$ mm^3 thick stone slabs. The test slab was placed on a cup which contained certain amount of water. The gap between the slab and the cup mouth was sealed by modeling clay, to ensure that water can only escape the cup through the pores in the stone slab. The mass loss of the water in the cup was recorded continuously and vapor diffusion coefficients μ was calculated from steady flow data by Eq. 3: [31]

$$\mu = (P \times \delta_L)/\left[\frac{M}{t \times S \times d}\right] \quad (3)$$

where μ is the vapor diffusivity (m^2 s^{-1}), P is the water vapor pressure (Pa) at test temperature. δ_L is the vapor constant in air (7.02×10^{-7} kg/m h^2 Pa). M is cup mass loss (kg) at time t (h), S is the cup mouth area (m^2), and d is the specimen thickness (mm). The larger the μ value is, the poorer the vapor permeability.

Color alteration was monitored by using the CIE Lab method according to the Italian Recommendation Normal [32]. Measured parameters included: L* for brightness, a* and b* for coordinates (a* being the red–green parameter and b* the blue–yellow one). For each formula of sol, four samples were analyzed at the same point before and after treatment. The CIE L*a*b color parameters were measured and total color difference ΔE was calculated by Eq. 4:

$$\Delta E = \left[(\Delta L^*)^2 + (\Delta a^*)^2 + (\Delta b^*)^2\right]^{0.5} \quad (4)$$

Resistance to salt cycles testing was carried out by impregnating the stone cubicles in a 16 wt% sodium sulfate solution for 7 h and then drying them at 60 °C in an oven for 15 h repeatedly [22]. The appearance and mass change of these cubicles were examined after each impregnating and drying cycle. Three treated stone samples ($20 \times 20 \times 20$ mm^3) were used for each consolidant. Mass loss reported was the average of measurements on three individual samples.

The aging resistance was evaluated by comparing the dynamic elastic modulus (E) after accelerated aging process, which was performed as following: 3 h at 250 °C followed by 3 h immersion in deionized water as one aging cycle [33]. Dynamic elastic modulus was measured after each aging cycle. Three treated stone samples ($20 \times 20 \times 200$ mm^3) were used for each consolidant. Elastic modulus reported was average of measurements on three individual samples.

3 Results and discussion

3.1 Consolidant characterization

3.1.1 Sol–gel process

Viscosity is an important parameter closely related to the mobility of consolidant sols inside the stone. As seen in Table 2, the addition of silica nanoparticles and PDMS-OH have increased the viscosities of the sols slightly, but all the consolidant sols have fairly small viscosities, i.e., they will all have excellent mobility inside the stone.

It seems that the addition of silica nanoparticles will accelerate the gelation due to the hydrogen bonding between hydrolyzed TEOS and silica nanoparticles [34]. It is known that with the increasing content of nano-SiO_2, the TEOS sol will lose its fluidity and reach the gelling point quickly. The PDMS alone seems to have small effect on the kinetics of the sol–gel process, while in the presence of silica nanoparticles, PDMS seems to weaken the acceleration effect of nanoparticles and slows down the gelation, probably due to the fact that there are only two hydroxyl groups on each PDMS molecule, much less than that of hydrolyzed TEOS and nano-SiO_2.

3.1.2 Bulky xerogels

The pictures of dried gels prepared in the test tubes are shown in Fig. 1. The gel network from the control sample collapses totally during drying, while gels from sols SP1 and P shrink during drying, but preserve their original shape, forming translucent to almost transparent silica monoliths. Although the gel from sol S does not collapse, the volume shrinkage is much more obvious than PDMS-containing sols and the gel is white, totally opaque. Apparently, very small amount of nanoparticles or PDMS addition will prevent the gel network from collapse.

Table 2 Viscosities of the consolidant sols

	Control	S	P	SP1	SP2	SP3
Viscosity (cP)[a]	1.64 ± 0.01	1.74 ± 0.01	1.72 ± 0.01	1.83 ± 0.01	1.80 ± 0.01	1.75 ± 0.01
Gel time	7 days	30 h	7 days	5 days	6 days	6 days

[a] Viscosity is the average of three individual measurements

Based upon the extent of volume shrinkage, it seems that PDMS works more efficiently than nano-SiO_2. More interestingly, SP1, in which both PDMS and nano-SiO_2 are introduced, has the smallest volume loss. It seems that there is some synergistic effect between PDMS and nano-SiO_2 particles which further minimize gel shrinkage. As for the monoliths from SP2 and SP3, they show very similar shrinkage and transparency to SP1 monolith.

3.1.3 Xerogel films

Based upon the applying technique and the nature of the stone, it is more possible that the consolidant exists in the form of film or coating inside the stone. Thus, in order to understand the consolidation process and outcome more closely to practical cases, consolidant xerogel films are also prepared in plastic dishes and carefully examined.

Fig. 1 Pictures of dried gels from various consolidant sols, from *left to right* SP1, S, P and control

The SEM images of the surface of the xerogel films formed by various sols are shown in Fig. 2. The control sol forms a dense nonporous film with severe cracking. The additions of PDMS and/or silica nanoparticles can significantly prevent crack formation in the films. As for the xerogel films from sols S and SP1, obvious pore structure can be observed, which is further convinced by BET data (Fig. 3; Table 3). Such pore structure will significantly reduce the capillary forces, thus minimize crack formation as the capillary force is inversely to the pore size [35]. In the cases of xerogel films from SP2 and SP3, their surfaces seem very rough as in S and SP1 samples, but the pore structures are much less obvious due to the lower nanoparticle contents.

On the other hand, the xerogel film from P sol is also very dense and proved to be nonporous by BET. It is known that the methyl groups in PDMS chains provide extra flexibility of its network. When introduced into silica network, the PDMS will make the gel network more flexible. Thus, it is possible that part of the stress generated during aging and drying can be released by the deformation/recovery of the network. Apparently, although both PDMS and nano-SiO_2 can prevent cracking in the silica gel network, they function via totally different mechanism. In SP series, both mechanisms may work simultaneously.

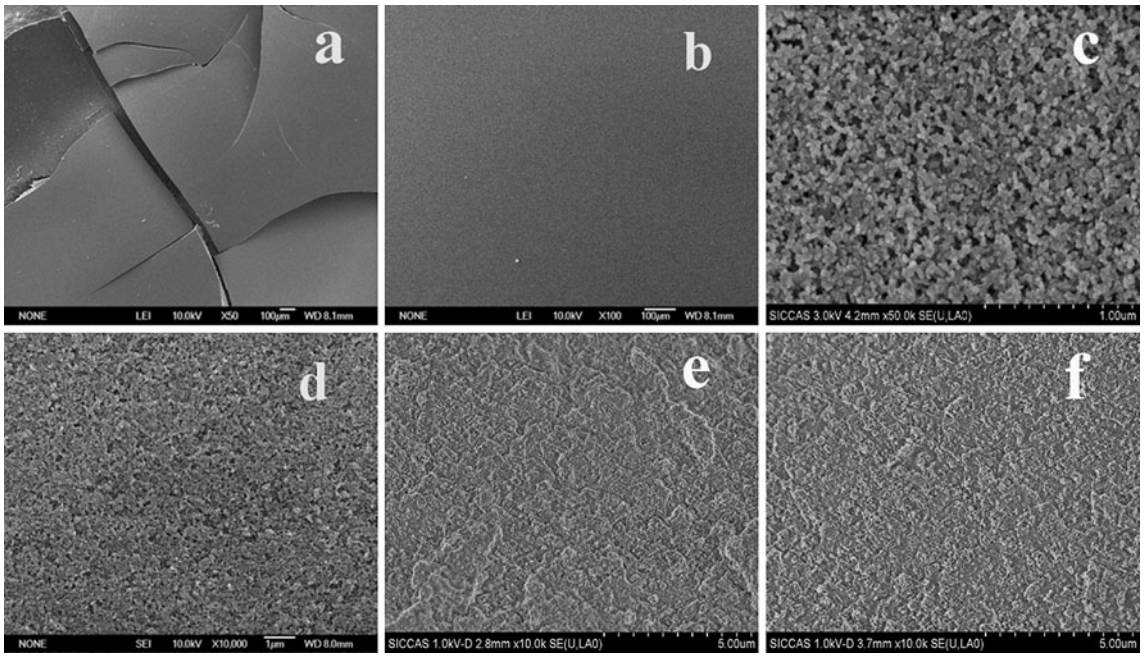

Fig. 2 SEMs of gels from different sols: **a** control, **b** P, **c** S, **d** SP1, **e** SP2 and **f** SP3

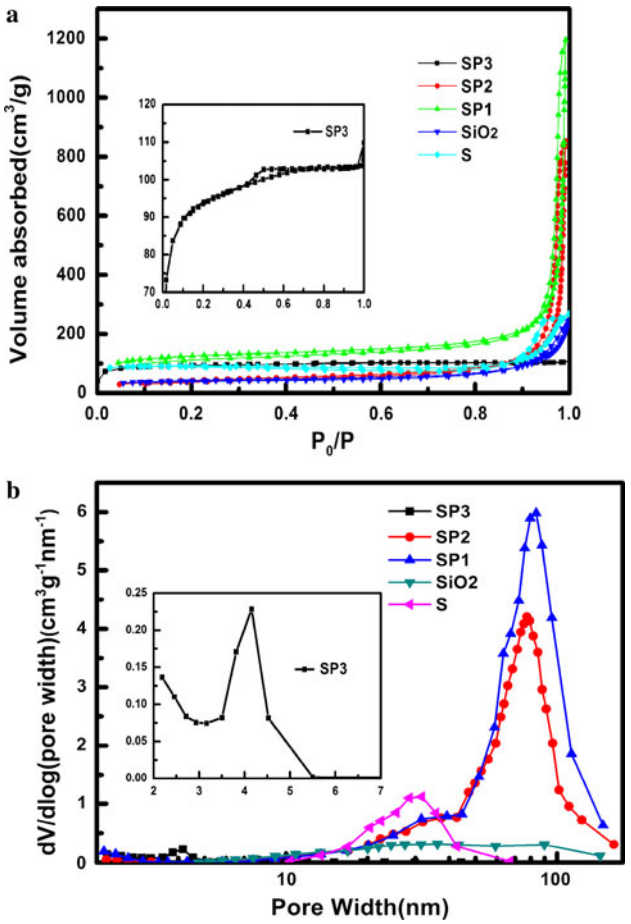

Fig. 3 **a** Nitrogen adsorption isotherms and **b** pore size distribution of the xerogels made from sols S, SP1, SP2, SP3 and nano-SiO_2. *Insets* data of xerogel from sol SP3

BET data shows that there is obvious porosity in the applied nano-SiO_2 particles with pore diameter ranging between 10 and 100 nm. Considering the particle size which is 15 nm, such porosity is most likely due to the stacking of particles. The pore volume detected is inter-particle voids [36]. Once the particles are dispersed in liquids, such pore volume disappears. Meanwhile, in Fig. 3b, the pores in nano-SiO_2-containing consolidant xerogels have very different diameter from that of nano-particles. So the pore structure detected in nano-SiO_2-containing consolidant xerogels is not coming from the nanoparticles or the stacking of the particles, but from the xerogel itself. It is known that faster gelation, for example sol–gel process in basic conditions, often leads to porous silica [37]. Nano-SiO_2 particles can accelerate the gelation like basic catalyst (obvious shorter gel time in Table 2) which may lead to the pore formation in the xerogels. It is reasonable to observe such porosity increases with nano-SiO_2 content (Table 3).

The function of PDMS in porosity is rather tricky. When only PDMS is brought into TEOS, the obtained xerogel is nonporous, which is not surprising at all. However, when both PDMS and nano-SiO_2 are introduced into TEOS, at the same nano-SiO_2 content of 4 wt%, the obtained xerogel has a porosity of 1.08 cm^3/g. Comparing to the xerogel from sol containing 4 wt% nano-SiO_2 only, the addition of 1 wt% PDMS unexpectedly increases the porosity more than three times. This is a strong evidence of the synergistic effect between PDMS and nano-SiO_2, which is probably due to the H-bonding interactions between the hydroxyl-terminated PDMS and nano-SiO_2. Considering the hydrophobic nature of TEOS (before hydrolysis), it is highly possible that the PDMS molecules are actually wrapping around the nano-SiO_2 particle surface instead of swimming freely in TEOS pool. PDMS molecules change the surface property of the nano-SiO_2 particles leading to much larger pore volume and pore size. Again the pore structure is introduced by nano-SiO_2, so when nano-SiO_2 content is reduced to 1 wt%, even though 1 wt% PDMS is added, the porosity becomes very low, only 0.06 cm^3/g (SP3 xerogel).

Table 3 Pore volume of xerogels from nano-SiO_2 containing sols

	SP1	SP2	SP3	S
Pore volume (cm^3/g)	1.08	1.06	0.06	0.32

The isotherms in Fig. 3a indicate that they are all typical type IV mesoporous materials, which is very often seen in silica gels [37]. Figure 3a shows that the xerogel from S sol have typical H2 type hysteresis loop, indicating possible ink-bottle shaped pores. While others show H3 hysteresis loop as evidenced by no limiting adsorption at high p/p°, indicating possible slit-like pores [38]. PDMS not only affects the pore volume, but also affects the pore shape strongly.

The films formed from control and P sols are transparent, while the film from S sol is opaque and whitish and the films from SP series are translucent. Combined with the results in bulky samples in Fig. 1, it is obvious that PDMS can also improve the transparency of the xerogels probably by reducing the scattering from the nanoparticles. PDMS may function as surfactant to mediate the interfacial difference between nano-SiO_2 and bulky gels [39].

3.2 Stone consolidation evaluation

The consolidant sols are applied on red sandstone and their conservation performance are examined carefully.

3.2.1 Physical properties

When consolidants are applied on the stone, many important properties of the stone, such as the pore structure,

water uptake, appearance etc. can be altered. It is vital to understand those changes before evaluate the effectiveness of consolidations.

The porosity data of the untreated and consolidant treated red sandstones, which are measured by MIP and gravimetric method respectively, are shown in Tables 4 and 5. MIP results show that for all the consolidants, before and after consolidation, there are no dramatic changes in stone's pore structure which is desired (Fig. 4). The bimodal pore size distribution in MIP data of both untreated and treated samples may relate to the different fissure modes as mercury intrusion [40]. The major difference in data from two methods is that in MIP method untreated sample has smaller porosity than treated ones while in gravimetric method it is the opposite [41]. It is possible that during MIP measurements, the high pressure (400 MPa) causes the thin wall of pores (or closed pores) to fracture which may lead to larger porosity. As for gravimetric method, two possible reasons may contribute to the smaller porosity. One is that the stone surface becomes less hydrophilic after treatment, thus may affecting the water wettability on the sample, which is supported by the contact angle changes. The other possible reason is that the consolidants partially fill the pores. But overall, data from both methods are pretty close and consistent.

The untreated sandstone is hydrophilic. It is known that water is the most important factor for stone deterioration because water is the media for recrystallization of soluble salts and freeze-thawing cycle which are responsible for most deterioration of the sandstones [42]. After treatments, the contact angles of water all increase notably, indicating the stone becomes less hydrophilic (Table 5). Both the nano-SiO_2 and PDMS can increase the contact angles over 100°, indicating hydrophobic surface and an improved resistance to wetting, which is beneficial to the stone conservation.

Acrylic based consolidant is commonly used in surface protection of culture heritage [43]. After applying acrylic based consolidants on stones, the hydrophobic nature of acrylics significantly improves the stone's resistance to wetting. Meanwhile, it is also found that the transportation of water within the stone decreases to a great extent after acrylics application [44], which is not good to the conservation. However, in Table 5, the data show that after consolidation treatment by our silicon based consolidants, the wettability of the treated stones decreases notably, while the transportation of water within the stone changes very slightly.

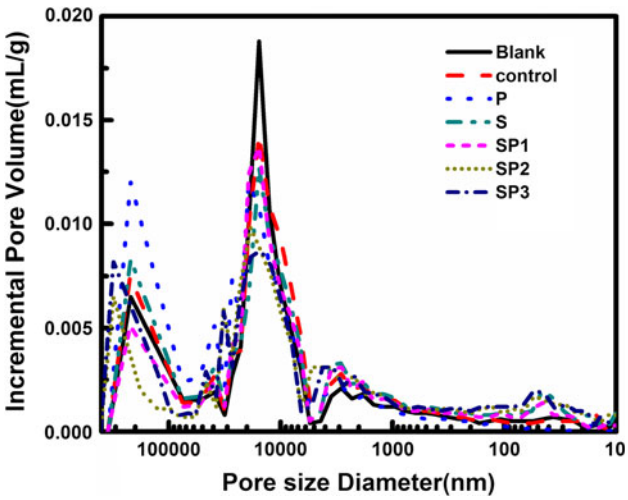

Fig. 4 Pore size distribution of untreated and treated (control, P, S, SP1, SP2 and SP3 sols) stone samples based on MIP

Table 4 Porosity of untreated and treated red sandstones based on MIP

	Untreated	Control	P	S	SP1	SP2	SP3
Porosity (%)	20.99	22.09	21.70	22.01	21.71	21.87	21.39

Table 5 Changes of physical properties of the red sandstone before and after consolidant treatment

	Water uptake (%)	Porosity (%)	Vapour diffusion coefficients (m^2 s^{-1})	Contact angle
Untreated	11.97 ± 0.22	24.18 ± 0.34	1.356 ± 0.021	/
Control	10.59 ± 0.12	21.60 ± 0.25	1.641 ± 0.033	25.8° ± 8.5°
S	10.68 ± 0.21	22.11 ± 0.28	1.692 ± 0.018	127.5° ± 3.6°
P	10.27 ± 0.05	21.11 ± 0.14	1.749 ± 0.015	133.5° ± 3.9°
SP1	10.32 ± 0.16	21.43 ± 0.22	1.781 ± 0.014	128.8° ± 2.1°
SP2	10.31 ± 0.11	21.38 ± 0.15	1.773 ± 0.011	130.5° ± 2.4°
SP3	10.29 ± 0.12	21.23 ± 0.18	1.758 ± 0.019	131.7° ± 4.1°

Data is average of individual measurements on 3 samples

3.2.2 Morphologies

The SEM picture of the partially deteriorated red sandstone is shown in Fig. 5a, in which large amount of pores and partially disaggregated clay particles can be clearly observed.

After the stone being treated with the consolidant sols, the sols penetrate into the pores and undergo sol–gel process. In the case of TEOS only (Fig. 5b, c), severe cracking of the gel can be observed in the fractured consolidated stone. Such cracking can be spread to the entire stone and totally destroy the whole object. Accelerated damage from water or salt can make such situation even worse [45]. When PDMS and/or nano-SiO_2 are introduced into TEOS, very nice crack-free gel phase can be obtained in the stone. In TEOS/PDMS case (Fig. 5d), the gel surface is quite smooth while in TEOS/PDMS/nano-SiO_2 case (Fig. 5f–h) the gel surfaces become rougher. In TEOS/nano-SiO_2 case, the gel surface is roughest and some particle agglomerates can be observed on the surface (Fig. 5e). It seems that PDMS can improve nano-SiO_2 dispersing more homogeneously in TEOS matrix. The roughness of the surface is apparently introduced by nano-SiO_2 and the roughness decreases as the nano-SiO_2 content decreases.

3.2.3 Consolidation and aging resistance evaluation

The major purpose of consolidant is to strengthen the stone. Table 6 lists compressive strength of the stone before and after treatment. After being applying on the stone, all

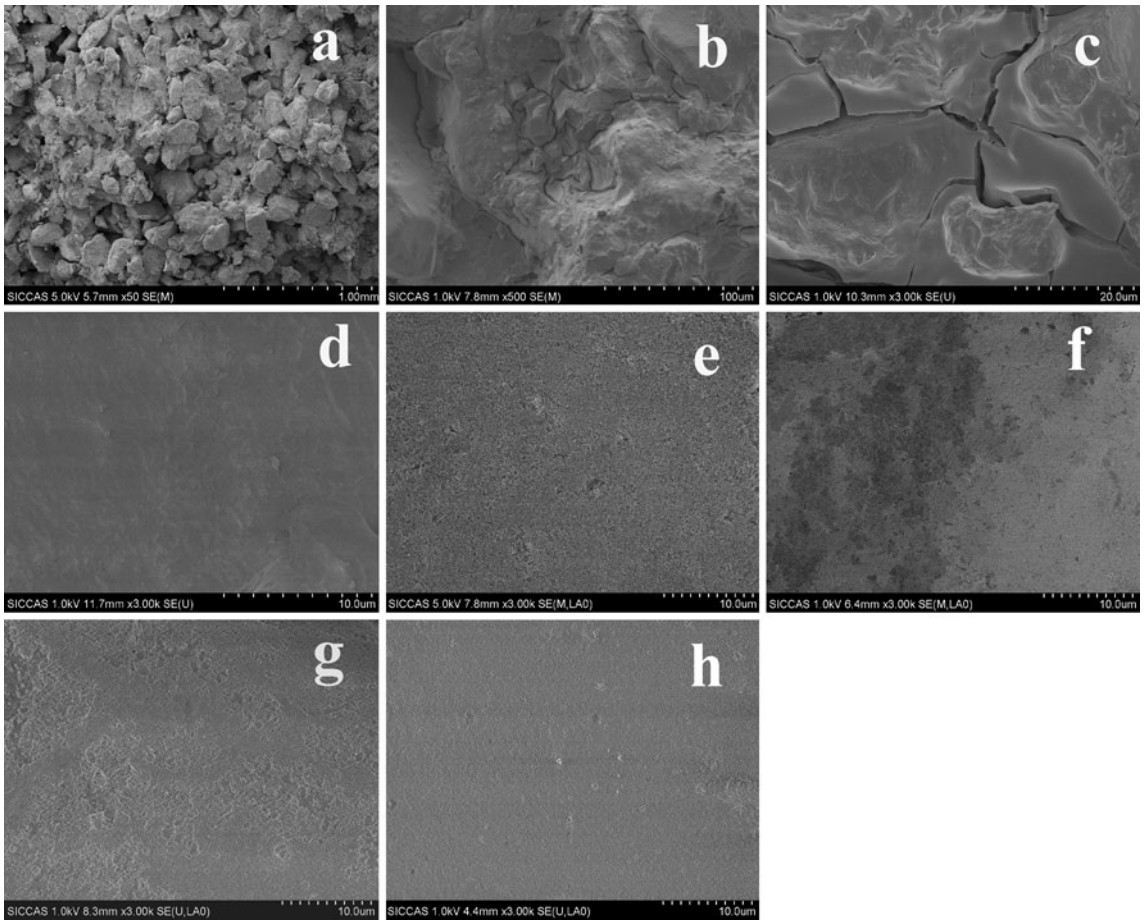

Fig. 5 SEM micrographs of fracture surface of the red sandstone of the Big Buddhist Temple **a** untreated, treated by **b**, **c** TEOS, **d** P, **e** S, **f** SP1, **g** SP2 and **h** SP3 sols

Table 6 Compressive strength of big Buddha temple sandstone treated by different consolidants

	Blank	Control	P	S	SP1	SP2	SP3
Strength (MPa)	12.8 ± 1.1	17.2 ± 0.8	13.3 ± 0.6	15.8 ± 1.2	14.2 ± 0.7	13.9 ± 0.7	13.5 ± 0.5

Data is average of individual measurements on 10 samples

consolidants show an increase in mechanical strength. Among those consolidants, TEOS (control) has the best consolidation ability. Sol S takes the second place. Sample P has the weakest consolidation ability due to the flexibility of PDMS. And it is reasonable to see that the consolidation ability of SP series decreases as nano-SiO_2 content decreases and basically it is a compromise of P and S.

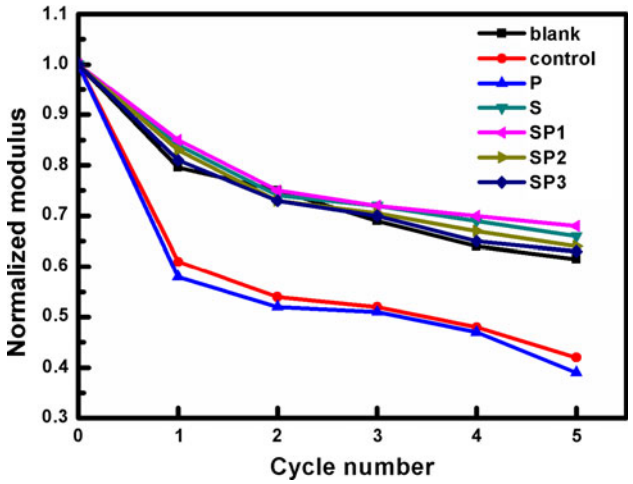

Fig. 6 Normalized dynamic elastic modulus loss of the blank sample and treated stones versus number of cycles in heat-aging cycles

The dynamic elastic modulus (E) can also be used to reflect the stone's mechanical strength. Since the measurement of E is non-destructive, this method can be used to track the aging process after consolidation. The relative change of E versus aging cycles is shown in Fig. 6. All samples exhibit decrease in E as the heat-aging process moving on. Comparing with blank, the heat-aging behaviors of TEOS (control) and P sols treated samples are deteriorated, while those of S and SP sols treated samples are improved. Samples treated by sol P show the biggest drop in E, only 40 % of the original value remained after intensive heat aging, probably due to the poor heat-aging resistance of PDMS. It appears that the three-component composite consolidant (SP1) shows best resistance to heat-aging, 70 % of the original modulus remained. Apparently, nano-SiO_2 can enhance the resistance to heat-aging process.

Salt resistance is another major cause for stone deterioration. Water soluble inorganic salts such as chlorides, sulfates will get access to the stone with underground

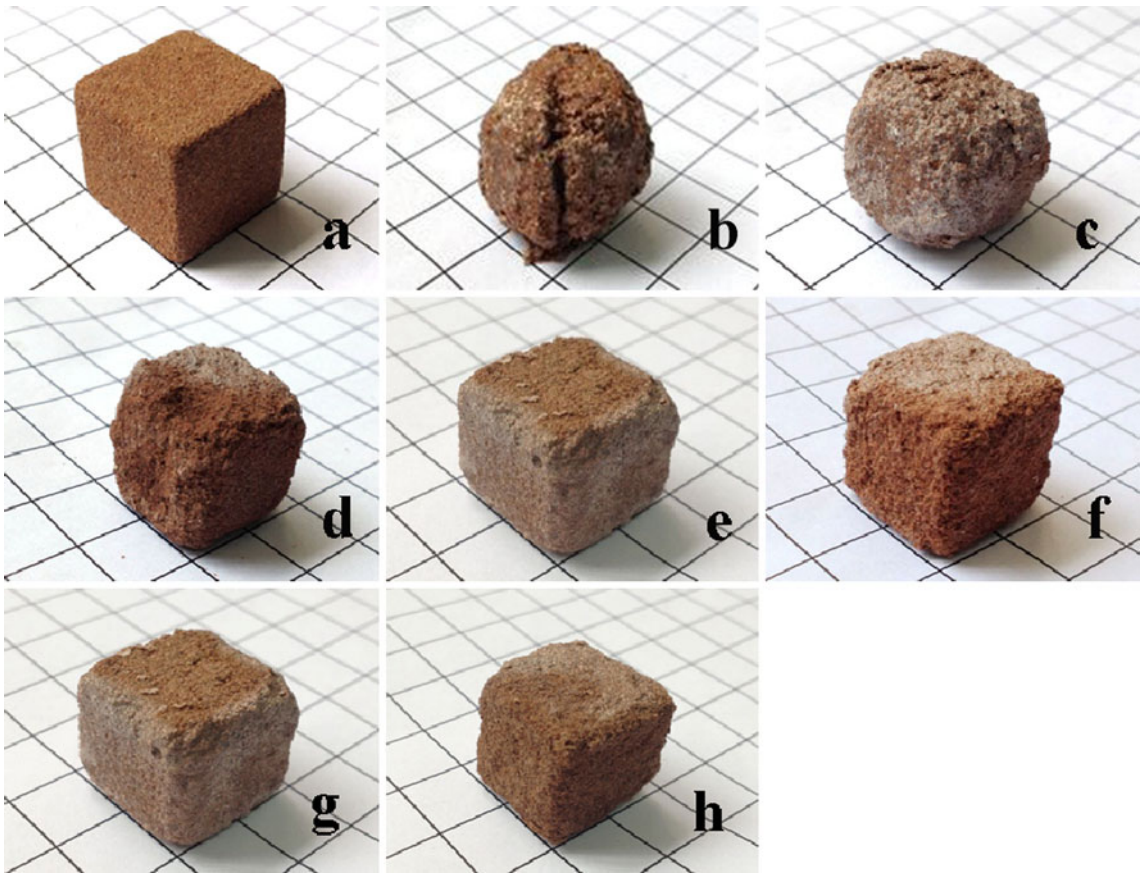

Fig. 7 **a** Original specimen, **b** untreated sample with 4 salt cycles; samples treated by sols: **c** control, **d** P, **e** S and **f** SP1, **g** SP2, **h** SP3 after 5 salt cycles

water. The salts recrystallize as water evaporates. The crystals will take up void space inside the stone grains and generate pressure upon the stone network. When that pressure outweighs the mechanical strength of the stone, the stone will deteriorate, in the form like loosing or cracking. Thus, improving salt resistance is highly desired in stone conservation.

Figure 7a is the picture of the original red sandstone. Figure 7b–f are the pictures of treated and untreated samples after four or five cycles of sodium sulfate test. Since

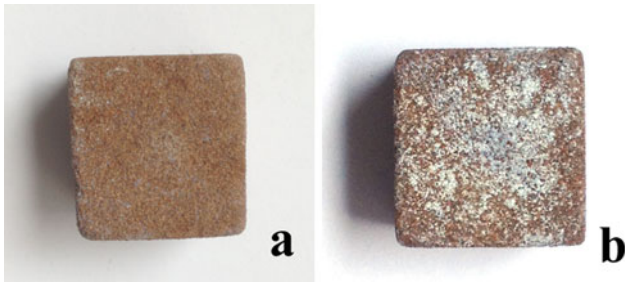

Fig. 10 Specimen **a** before and **b** after treated by S sol

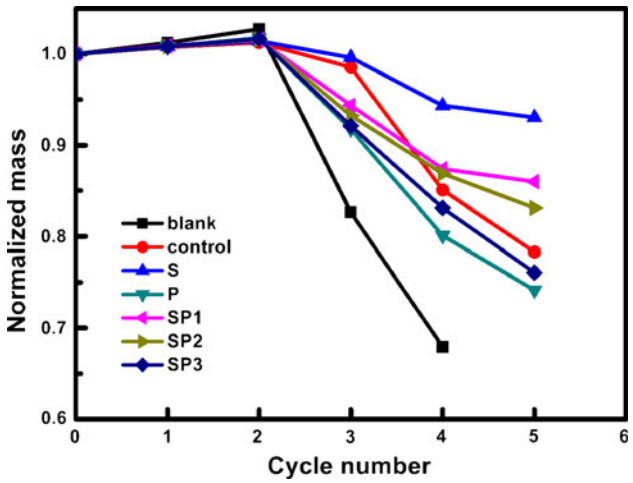

Fig. 8 Normalized mass loss of the stones versus number of cycles in sodium sulfate test

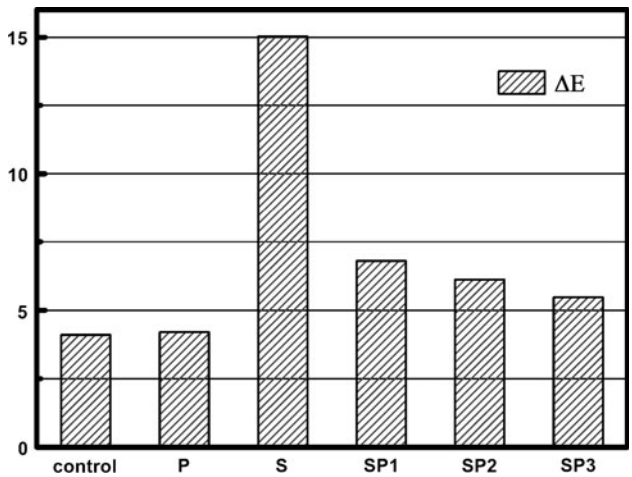

Fig. 11 Color alteration of treated sandstones samples by different consolidants

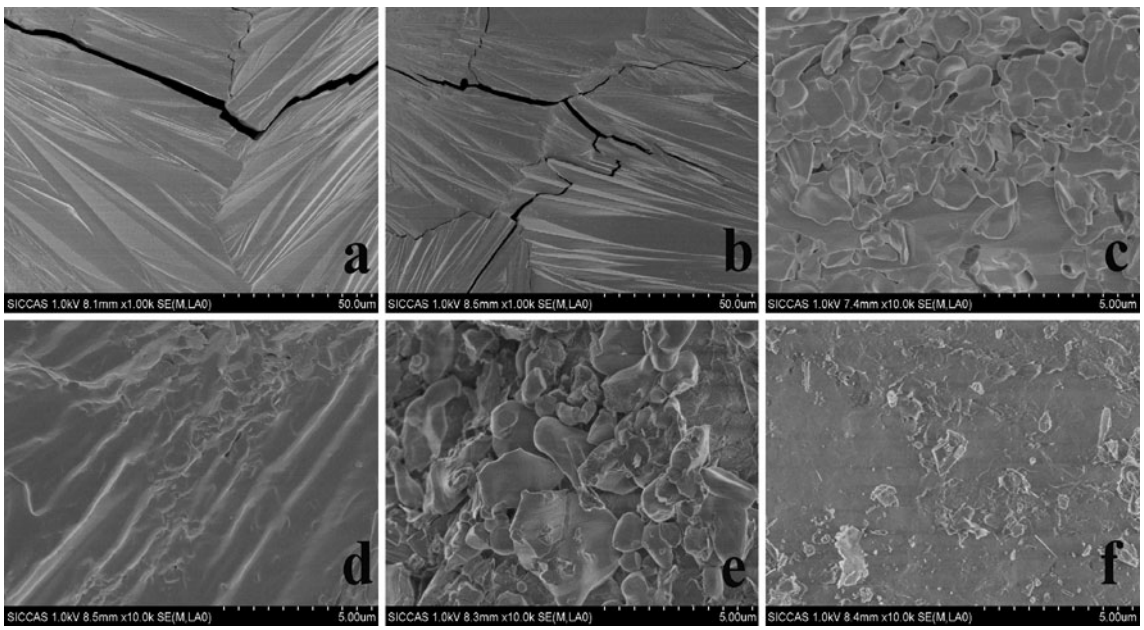

Fig. 9 SEM images of TEOS-based sols treated sandstone after 5 cycles of salt test. Samples treated by **a** control, **b** P, **c** S, **d** SP1, **e** SP2 and **f** SP3 sols

Table 7 Overall consolidation evaluation of TEOS-based consolidants

	Crack-free	Strength (MPa)	Heat-aging resistance	Salt resistance[a]	Color alteration (ΔE)
Untreated	/	12.8	Good	7	/
Control	Poor	17.2	Poor	4	4.1
S	Good	15.8	Good	1	15.0
P	Good	13.3	Poor	6	4.2
SP1	Good	14.2	Good	2	6.8
SP2	Good	13.9	Good	3	6.1
SP3	Good	13.5	Good	5	5.5

[a] 1 for the best resistance, 7 for the worst

the untreated sandstone sample totally breaks into pieces after 5 wet–dry cycles, the picture after 4 cycles is shown in Fig. 7b. As for samples treated by TEOS and P sols, severe damage can be observed after 5 wet–dry cycles (Fig. 7c, d). As strong comparisons, samples treated by silica nanoparticles containing sols (S, SP1, SP2 and SP3 sols) still remain their original shapes. It can be clearly seen that untreated sandstone and the sandstones treated by TEOS and P sols show very poor resistance to salts, while the stone's salt resistance is significantly enhanced after being treated by S and SP series sols.

For each consolidant applied, the average weight loss of three stone samples after each wet–dry cycle are recorded and plotted in Fig. 8. For all samples, they actually gain weight in the first two cycles due to the absorption of the salt. The blank sample gains most because it is hydrophilic and could absorb more water than treated samples, thus absorb more salts. The water uptake ability of treated samples are pretty close (see Table 5), so their weight gains are also similar. The mass curves begin to decline from the third cycle because grains start to loose from the bulk due to the salt crystallization. Among all the curves, it seems that the sample treated by S sol has the best salt resistance, followed by the sample treated by SP1 sol. It is worth noting that the salt resistance of the sample treated by P sol is even worse than that of the samples treated by TEOS only, which suggests that we should be very cautious when applying PDMS in stone conservation. Figures 7 and 8 show that nano-SiO_2 particles can enhance the stone's resistance to salt notably. And such ability depends upon the nanoparticle's content. The higher the particle content, the better salt resistance can be obtained.

Figure 9 shows the SEM pictures of the surface of the fractured consolidated samples after 5 wet–dry cycles. In the samples treated by control and P sols, large rod-like crystals can be observed as well as huge cracks. On the other hand, for samples treated by S and SP series, no such huge rod-like crystals and cracks can be seen. It seems that nano-SiO_2 suppress the large rod-like crystal formation possibly due to seeding effect [46].

3.2.4 *Color alteration*

Measurements are carried out before and after the treatment on stone samples. Generally, a slight color change ($\Delta E < 5$) resulting from the restoration is accepted [24]. However, there is visible appearance change on the sample treated by S sol (Fig. 10), due to the scattering of the nanoparticles, with ΔE as high as 15.03. This is not a big surprise since the gel or film prepared from this sol is white, totally opaque.

The ΔE values of treated samples are summarized in Fig. 11. Samples treated with control and P sols have no notable change in visual appearance with $\Delta E < 5$. For samples treated by SP series, it is obvious that PDMS can significantly reduce the color change probably by weakening the scattering from nanoparticles and preventing nanoparticle agglomeration. When the nanoparticle content is 1 %, with the help of PDMS, the color change of the sample can drop into an acceptable range ($\Delta E = 5.47$).

4 Conclusions

Tetraethoxysilane is a commonly used stone consolidant. It forms Si–O network after sol gel process, which functions as the binder to strengthen the stone. But the gel generated from TEOS alone often cracks, leading to more serious damage to the stone. The addition of PDMS or nano-SiO_2 can reduce the risk of crack formation after consolidant material being applied on the stone. Unfortunately, PDMS can also lead to poorer aging resistance, especially heat-aging and salt resistance, while nano-SiO_2 brings unacceptable color alteration.

In order to solve the cracking issue without bringing new problems, TEOS-based three-component stone consolidants are prepared by sol–gel process. The composite consolidants consist of 15 nm silica particles, α,ω-hydroxyl-terminated polydimethylsilane (PDMS-OH) and TEOS. In this system, due to the hydrophobic nature of TEOS (before hydrolysis), the hydroxyl-terminated PDMS molecules tend to stay on the

hydrophilic surface of nano-SiO_2. By wrapping around the nanoparticles, PDMS not only prevents the particle from agglomeration, but also functions as a bridge to mediate the interfacial difference between nano-SiO_2 and bulky gels. Thus PDMS significantly reduces the color alteration caused by nano-SiO_2. Due to the synergistic effects with PDMS, the three-component composite also has smallest volume shrinkage and best heat-aging resistance, even better than TEOS/nano-SiO_2 system.

In general, by the synergistic effect among the three components, the three-component composite stone consolidant exhibits the best overall performance which is summarized in Table 7.

Acknowledgments The authors would like to thank Professor He Ling and her research group from Xi'an Jiaotong University for helping us obtaining the stone samples. The authors are also grateful for the financial support from the 973 National Key Basic Research and Development Program (2012CB720904) and the Hundred Talents Program of the Chinese Academy of Science.

References

1. Hansen E, Doehne E, Fidler J et al (2003) Rev Conserv 4:13–25
2. Watt D, Colston B (2000) Build Environ 35:737–749
3. Wheeler G (2005) Alkoxysilanes and the consolidation of stone. Getty Publications, Los Angeles
4. Zendri E, Biscontin G, Nardini I, Riato S (2007) Constr Build Mater 21:1098–1106
5. Grissom C, Charola AE, Boulton A, Mecklenburg F (1999) Stud Conserv 44:113–120
6. Scherer GW, Wheeler G (2009) Key Eng Mater 391:1–25
7. Miliani C, Velo-Simpson ML, Scherer GW (2007) J Cult Herit 8:1–6
8. Minami T (2011) J Sol–Gel Sci Technol 9:1–8
9. Brinker CJ, Scherer GW (1990) Sol–gel science. Academic Press, New York
10. Brus J, Kotlik P (1996) Stud Conserv 41:324–332
11. Mosquera MJ, Pozo J (2003) J Sol–Gel Sci Technol 26:1227–1231
12. Mosquera MJ, Bejarano M, Rosa-Fox N, Esquivias L (2003) Langmuir 19:951–957
13. Zarraga R, Cervantes J, Salazar-Hernandez C, Wheeler G (2010) J Cult Herit 11:138–144
14. Antonietti M, Berton B, Goltner C, Hentze HP (1998) Adv Mater 10:154–159
15. Mosquera MJ, de los Santos DM, Montes A (2008) Langmuir 24:2772–2778
16. Xu FG, Li D, Zhang HA, Peng W (2012) J Sol–Gel Sci Technol 61:429–435
17. Yang M, Scherer GW, Wheeler G (1998) In: Compatible materials for the protection of European cultural heritage, Athens, PACT 56:201–208
18. Alie C, Pirard R, Lecloux AJ, Pirard JP (1999) J Non Cryst Solids 246:216–228
19. Scherer GW, Flatt R, Wheeler G (2001) MRS Bull 26:44–50
20. Escalante MR, Flatt R, Scherer GW et al (2002) In: Protection and conservation of the cultural heritage of the Mediterranean cities, Netherlands, pp 425–429
21. De Ferri L, Lottici PP, Lorenzi A et al (2011) J Cult Herit 12: 356–363
22. Aggelakopoulou E, Charles P, Acerra ME et al (2002) In: Materials issues in art & archaeology VI. MRS Symposium Proc, pp 712–725
23. Sasse HS, Snethlage R (1996) In: Methods for the evaluation of stone conservation treatments. Report of Dahlem workshop on saving our architectural heritage, Berlin, p 225
24. Mackenzie JD (1994) J Sol–Gel Sci Technol 2:458–469
25. Wendler E, Klemm DD, Snethlage R (1991) In: Consolidation and hydrophobic treatment of naturalstone, Proceedings of fifth international conference on durability of building materials and components, Brighton
26. Grassien N, MacFarlane IG (1978) Eur Polym J 14:875–884
27. Mosquera MJ, de los Santos DM, Rivas T (2010) Langmuir 26: 6737–6745
28. Pinto AP, Rodrigues JD (2008) J Cult Herit 9:38–53
29. ASTM C170/C170M-09 (2009) Standard test method for compressive strength of dimension stone. ASTM International, West Conshohocken. doi:10.1520/C0170_C0170M-09
30. ASTM C97/C97M-09 (2009) Standard test methods for absorption and bulk specific gravity of dimension stone. ASTM International, West Conshohocken. doi:10.1520/C0097_C0097M-09
31. Al-Saad Z, Abdel-Halim MAH (2001) Eng Struct 23:926–933
32. NorMal. 43/93 (1994) Misure colorimetriche per superfici opache. CNR-ICR, Roma
33. Sassoni E, Naidu S, Scherer GW (2011) J Cult Herit 12:346–355
34. Park JT, Lee KJ, Kang MS (2007) J Appl Polym Sci 106: 4083–4090
35. Escalante M, Valenza J, Scherer GW (2000) In: 9th International conference on the deterioration and conservation of stone. Elsevier, Amsterdam, pp 459–460
36. Stanley-Wood NG, Johansson ME (1980) Analyst 105:1104–1112
37. Colomer MT, Anderson MA (2001) J Non Cryst Solids 290: 93–104
38. IUPAC (1982) Pure Appl Chem 54:2201–2218
39. Chen XC (2002) J Mater Sci Lett 21:1637–1639
40. Mosquera MJ, Rivas T, Prieto B, Silva B (2000) J Colloid Interf Sci 222:41–45
41. Mosquera MJ, Pozo J, Esquivias L (2003) J Non Cryst Solids 26:334–343
42. He L, Liang G, Wu Y (2003) Mater Rev (Engl Transl) 17:82–84
43. Alessandrini G, Aglietto M, Castelvetro V et al (2000) J Appl Polym Sci 76:962–977
44. Basheer PAM, Basheer L, Cleland DJ, Long AE (1997) Constr Build Mater 11:413–429
45. Scherer GW (1999) Cem Concr Res 29:1347–1358
46. Towata A, Hwang HJ, Yasuoka M, Sando M (2000) J Mater Sci 35:4009–4013